



## A novel biosensor based on hafnium oxide: Application for early stage detection of human interleukin-10

Michael Lee<sup>a,\*</sup>, Nadia Zine<sup>a</sup>, Abdellatif Baraket<sup>a</sup>, Miguel Zabala<sup>b</sup>, Francesca Campabadal<sup>b</sup>, Raffaele Caruso<sup>c</sup>, Maria Giovanna Trivella<sup>d</sup>, Nicole Jaffrezic-Renault<sup>a</sup>, Abdelhamid Errachid<sup>a</sup>

<sup>a</sup> Université de Lyon, Université de Claude Bernard Lyon1, Institut de Sciences Analytiques (ISA) – UMR 5280, 43 Boulevard du 11 Novembre 1918, 69622 Villeurbanne Cedex, France

<sup>b</sup> Instituto de Microelectrónica de Barcelona (IMB), Centro Nacional de Microelectrónica (CNM) – CSIC, 08193 Bellaterra, Barcelona, Spain

<sup>c</sup> CNR (Consiglio Nazionale Ricerche) Clinical Physiology Institute, Niguarda Cà Granda Hospital, P.zza Ospedale Maggiore 3, 20162 Milan, Italy

<sup>d</sup> CNR (Consiglio Nazionale Ricerche) Clinical Physiology Institute, Via Moruzzi 1, 56124 Pisa, Italy

### ARTICLE INFO

#### Article history:

Available online 22 May 2012

#### Keywords:

Biosensor  
Hafnium oxide  
Aldehyde  
Electrochemical impedance spectroscopy  
Microcontact printing  
Interleukin-10

### ABSTRACT

Measurement of interleukin-10 (IL-10) has subsequently become a crucial tool to identify end-stage heart failure (ESHF) patients prone to adverse outcomes during the early phase of left ventricular assisted device (LVAD) implantation. In this context, label-free detection using a novel substrate based on hafnium oxide (HfO<sub>2</sub>) grown by atomic layer deposition (ALD) on silicon was applied. Here, we studied the interaction between recombinant human (rh) IL-10 with the corresponding monoclonal antibody (mAb) for early cytokine detection of an anti-inflammatory response due to LVAD implantation. For this purpose, HfO<sub>2</sub> has been functionalized using an aldehyde–silane ((11-(triethoxysilyl) undecanal (TESUD)) self-assembled monolayer (SAMs), to directly immobilize the anti-human IL-10 mAb by covalent bonding. The interaction between the antibody–antigen (Ab–Ag) was characterized by fluorescence patterning and electrochemical impedance spectroscopy (EIS). Confirmation for the bio-recognition of the protein was achieved by fluorescence patterning, while Nyquist plots have shown a stepwise variation due to the polarization resistance ( $R_p$ ) between the Ab activated surfaces with the detection of the protein. For early expression monitoring, commercial proteins of rh IL-10 were analyzed between 0.1 pg/mL and 50 ng/mL. Protein concentrations within the linear range of 0.1–20 pg/mL were detected, and these values formulated a sensitivity of 0.49 (ng/mL)<sup>-1</sup>. These preliminary results demonstrated that the developed biosensor was sensitive to the detection of rh IL-10, and the measured limit of 0.1 pg/mL in phosphate buffered saline (PBS) was clearly detectable, which displays the high sensitivity of EIS. On analysis of an interference attributable to non-specific binding of other cytokine biomarkers; tumor necrosis factor- $\alpha$  (TNF- $\alpha$ ) and IL-1 $\beta$  were analyzed without causing an interference to the IL-10 mAb. This established that selective sensitivity was responsive only to rh IL-10. To our knowledge, this is the first biosensor that has been based on HfO<sub>2</sub> for Ag detection by EIS. In time, the HfO<sub>2</sub> insulator will be incorporated into the gate of silicon-based ion-sensitive field-effect transistors (ISFETs) and developed as a portable real time detection system for the IL family of biomarkers in human serum.

© 2012 Elsevier B.V. All rights reserved.

### 1. Introduction

Heart failure (HF) has become a huge problem in the western world. Every year, approximately 1 million new patients are diagnosed with this illness, which makes it one of the fastest growing cardiovascular diseases (CVDs). Various commonly available methods for the detection of biomarkers related with CVDs have been developed, such as immunoaffinity column assay, fluorometric,

and enzyme-linked immunosorbent assay (ELISA) [1–5]. However, these laboratory techniques are based on sophisticated instrumentation that requires qualified personnel, while sample preparation and analysis are also time consuming. Therefore, there is an urgent need for easier use of diagnostic tools with high sensitivity and selectivity, which enable identification of the severity of the inflammatory state in the early stages and thus permit early therapeutic intervention. Such tools would be of great help to treat HF before the patients quality of life is compromised and hence, aid in the development of new pharmacotherapeutic options.

Biosensors based on electrical measurement are devices that employ biochemical molecular recognition for desired selectivity with a specific biomarker of interest. Such biosensors present a

\* Corresponding author. Tel.: +33 4 72 43 14 44; fax: +33 4 72 44 84 79.

E-mail addresses: [michael.lee@etu.univ-lyon1.fr](mailto:michael.lee@etu.univ-lyon1.fr) (M. Lee), [abdelhamid.errachid@univ-lyon1.fr](mailto:abdelhamid.errachid@univ-lyon1.fr) (A. Errachid).

system that is sensitive, label-free, rapid, reproducible, portable, and at low production costs can eliminate applications that utilize time-consuming laboratory equipment [6–10]. Recently, it has been used for the detection of IL-6 and IL-8 with very low concentrations measured [11,12].

In general, biosensor fabrication is based upon the semiconducting properties of silicon with thermally grown silicon dioxide ( $\text{SiO}_2$ ) and silicon nitride ( $\text{Si}_3\text{N}_4$ ) being most favored over the past decades, when applied as transistor gates within field effect transistors (FETs) [13–17]. With the thickness reduction of  $\text{SiO}_2$  complementary metal oxide semi-conductor (CMOS) devices, high gate oxide leakage becomes apparent as the reliability of the  $\text{SiO}_2$  layer is jeopardized. Capacitance can be improved by increasing the dielectric constant ( $K$ ) without having to reduce the dielectric thickness to leaky dimensions. Many other materials have been considered as potential alternatives for high- $K$  gate materials instead of  $\text{SiO}_2$  as they present the necessary capacitance due to physical thickness and a reduction of the gate leakage current [18]. These include: aluminum oxide ( $\text{Al}_2\text{O}_3$ ), tantalum pentoxide ( $\text{Ta}_2\text{O}_5$ ), titanium dioxide ( $\text{TiO}_2$ ), zirconium dioxide ( $\text{ZrO}_2$ ) and hafnium oxide ( $\text{HfO}_2$ ) [19–25]. One of these extensively researched materials is  $\text{HfO}_2$ . When compared to the aforementioned high- $K$  dielectrics,  $\text{HfO}_2$  has increased thermal stability on silicon by using atomic layer deposition (ALD) as deposition method ( $\text{Al}_2\text{O}_3$  has also improved stability on Si, but a lower  $K$  of 9 does not render it beneficial for capacitor applications in the continued CMOS advancements), and a higher  $K$  for reduced leakage and enhanced gate capacitance when compared with  $\text{SiO}_2$  [23]. Therefore,  $\text{HfO}_2$  can be considered a promising high- $K$  gate material. On application to a biosensor, these properties can be addressed when considering the charge effect of a material. For instance, improved thermal stability creates a good interface for electrical performance, since consistent capacitance switching behavior of the semiconducting channel correlates to the gate oxide layer that is deposited on the channel [25], while, relative activation requirements upon functionalization of a surface can also be improved by application of a high- $K$  material that obtains a highly polar surface (e.g. low  $K$  materials require aggressive activation to improve chemical bonding of the required silane, e.g. piranha solution).

Recently, Chen et al. have applied  $\text{HfO}_2$  as a highly sensitive bio-field-effect transistor (bioFET) for biotin functionalization using capacitance–voltage measurements [25]. Streptavidin binding was reproducible by application of a linker molecule; (3-aminopropyl)triethoxysilane (APTES). The authors have demonstrated that  $\text{HfO}_2$  can be applied for functionalization with biomolecules and, therefore, we propose the first novel  $\text{HfO}_2$  biosensor that has been functionalized for antibody (Ab) deposition with detection of a human antigen (Ag) by electrochemical impedance spectroscopy (EIS).

IL-10 is an anti-inflammatory cytokine with an important role in modulating the inflammatory processes in several diseases related with inflammation. An exacerbated increase of IL-10, in addition to uncontrolled release of pro-inflammatory mediators, was proposed as a peculiar pattern of adverse inflammatory response related to the magnitude of multi-organ dysfunction in end-stage heart failure (ESHF) patients supported by left ventricular assisted device (LVAD) [2]. In the early phase of LVAD support, patients are more susceptible to adverse events and are at a higher risk of multiple organ failure syndrome (MOFS). The impact of MOFS, ultimately leads to mortality of the patient and it is influenced by the degree of immuno-inflammation [2]. As a cause, this factor is independent of infection, and the inflammatory response is most dangerous during the first month, especially, within the first few hours after implantation. Early expression of IL-10 within the pg/mL range can discriminate patients of high risk, and since EIS is rapid, early therapeutic intervention can be provided by the clinicians to assist

in preventing MOFS from developing to a critical stage. Stumpf et al. reported CHF IL-10 plasma cytokine levels for 50 patients at  $2.3 \pm 1.9$  pg/mL, while controls were measured at  $5.2 \pm 2.3$  pg/mL ( $P < 0.01$ ) [26]. Finally, Bolger et al. studied plasma IL-10 cytokine levels where CHF patients were recorded at  $3.7 \pm 1.1$  pg/mL and control patients at  $4.9 \pm 1.5$  pg/mL ( $P = 0.50$ ) [27]. These results demonstrated plasma samples from CHF patients that had not undergone LVAD implantation though were classified with this condition. Here, the severity of CHF levels was classified as New York Heart Association (NYHA) class II to IV [26], though on both accounts, the control patients recorded an increase in IL-10 plasma levels.

In a study of patients who underwent surgery for LVAD implantation, Caruso et al. have reported detectable human IL-10 plasma levels for 23 LVAD implanted patients between a range of 0 and 1558 pg/mL in the first 30 days of LVAD support using ELISA [2]. Interestingly, the authors analyzed samples within certain time frames to quantify exactly when patients were susceptible to higher levels of inflammation after surgery. Before LVAD implantation, patients obtained minimal IL-10 inflammation (pre-implant) due to the circulating cytokine (1-month survivors, 1.8 pg/mL and non-survivors, 5.6 pg/mL). Following LVAD implantation, plasma samples were taken after 4 h. At this critical stage, early expression of human IL-10 peaked in comparison with other plasma samples analyzed within the 30 day period for survivors and non-survivors. Levels for IL-10 non-survivors (177.8 pg/mL) were also higher than that of the survivors (56.2 pg/mL). Therefore, the authors have established that the elevated IL-10 levels in parallel with other cytokines can play an important role in the development of adverse events early after LVAD implantation [2,3].

Here, we present a novel substrate of  $\text{HfO}_2$  where the surface has been functionalized with 11-(triethoxysilyl) undecanal (TESUD) by chemical vapor deposition in a saturated medium [28,29]. Surface activation has enabled direct monoclonal antibody (mAb) bonding, where no other reagents were required that could in essence denature the primary capture Ab [28]. Surface treatment was analyzed by contact angle measurements (CAM) that were based upon cleaned, UV/Ozone activated and TESUD surfaces. The Ab–Ag–Ab bio-recognition on  $\text{HfO}_2$  TESUD activated substrates was characterized by fluorescence microscopy, while application of EIS aided in the evaluation of this novel biosensor for early stage detection of human IL-10 inflammation for LVAD recipients.

## 2. Materials and methods

### 2.1. Process for substrate fabrication

In the ALD technique, very thin layers can be deposited by sequential self-terminating gas–solid reactions. The cyclic nature of this deposition process results in a layer-by-layer deposition, which exhibits a very important advantage in terms of both thickness and composition control. Typically, a deposition cycle in that sequence, consists on the introduction of the first appropriate precursor gas into the reaction chamber in the form of a very short time pulse, producing the chemisorption of the precursor onto the surface of the substrate, followed by a purge step with an inert gas to remove the precursor excess and the reaction by-products; next, the second precursor gas is pulsed and introduced into the chamber and reacts with the first precursor present on the substrate; and, finally, another purge step is done with the same purpose of the first one. This constitutes one cycle of the process and a monolayer growth by cycle is obtained due to the self-limiting nature of the reactions.

The samples structures were made on 100 mm-diameter p-type silicon wafers (100), oriented with a resistivity of 4–40  $\Omega$  cm.

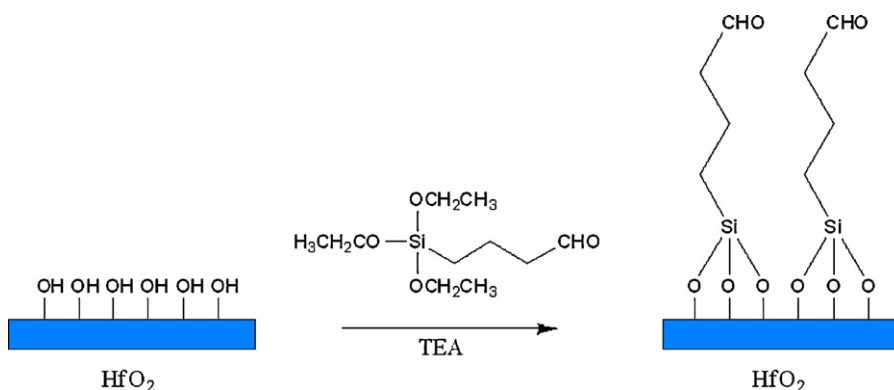


Fig. 1. Surface activation on  $\text{HfO}_2$  by UV/Ozone followed by vapor deposition in a saturated medium of TESUD.

After standard cleaning, the high- $K$  dielectric was deposited by the ALD as described before. We have used the Savannah-200 ALD system set up at IMB-CNM, which consists of a thermal ALD system at a controlled temperature and under vacuum. The system uses deionized  $\text{H}_2\text{O}$  as the oxygen precursor, together with tetrakis(dimethylamido)-hafnium for  $\text{HfO}_2$  deposition and  $\text{N}_2$  as the carrier/purging gas. Deposition of the  $\text{HfO}_2$  layer was carried out at a temperature of  $225^\circ\text{C}$  and at a base pressure of 300 mTorr using 100 ALD cycles. A first estimation of the deposited  $\text{HfO}_2$  layer thickness was carried out by means of ellipsometry, obtaining a thickness of 10.7 nm having fixed the refractive index to 2.07. Finally, a 500 nm-thick aluminum layer was deposited on the back of the wafers for electrically contacting the silicon substrate. For more information concerning the effects of processing conditions and electrical characteristics, see [19,20].

## 2.2. Fluorescent imaging of functionalized TESUD substrates with Ab–Ag–Ab bio-recognition

Bare  $\text{HfO}_2$  substrates were cleaned by sonication in acetone for 10 min, followed by thorough rinsing in ultrapure water (Millipore Milli-Q). Surface activation of the  $\text{HfO}_2$  substrates was performed using an UV/Ozone Procleaner™ (BioForce, Germany) for 20 min. Afterwards, the substrates were thoroughly rinsed and sonicated in Milli-Q water for 10 min. The  $\text{HfO}_2$  substrates were functionalized by a SAMs of TESUD (Gelest, USA) using vapor-phase method for 1 h (Fig. 1). This activation technique has been recently reported by Caballero et al. [28,29] where  $\text{Si}_3\text{N}_4$  surfaces have been aldehyde-functionalized for the detection of human serum albumin (HSA). Finally, the substrates were placed into an oven at  $100^\circ\text{C}$  for 1 h, and after baking, the substrates were rinsed in absolute ethanol and dried with nitrogen.

A positive  $10\ \mu\text{m}$  structured polydimethylsiloxane (PDMS) stamp was cleaned by sonication in absolute ethanol for 10 min. A solution of anti-human IL-10 mAb ( $10\ \mu\text{g}/\text{mL}$ ) (R&D Systems, France) was physisorbed onto the PDMS stamp for 20 min and then dried with nitrogen. The stamp was positioned onto the  $\text{HfO}_2$  TESUD substrates and microcontact printing ( $\mu\text{CP}$ ) was maintained for 10 min (Fig. 2a) using an automated microcontact printer ( $\mu\text{CP}$  3.0 GeSiMs, Germany). The substrates were rinsed in phosphate buffered saline (PBS) (pH 7.4) (Sigma–Aldrich, France) and dried with nitrogen.

After the deposition of the mAb, the non-functionalized regions were blocked using a 1 mM triethylamine (Sigma–Aldrich, France) solution of alpha-methoxy-omega-amino poly(ethylene glycol) ( $\text{MeO-PEG-NH}_2$ ) (Iris Biotech GmbH, Germany) for 30 min (Fig. 2b). After this time, the samples were rinsed in PBS and dried with nitrogen.

Subsequently, the substrates were incubated with human IL-10 protein (R&D Systems, France) ( $0.25\ \mu\text{g}/\text{mL}$ ) for 1 h. This allowed the Ab–Ag interaction to formulate (Fig. 2c). After that, the samples were rinsed in PBS and dried with nitrogen.

Finally, the substrates were incubated with anti-human IL-10-Fluorescein mAb (R&D Systems, France) ( $2.5\ \mu\text{g}/\text{mL}$ ) for 1 h (Fig. 2d), to complete the final affinity. The samples were rinsed in PBS, then dried with nitrogen, and observed using a fluorescence microscope (Zeiss Axio Scope.A1, France).

## 2.3. Detection of varying rh IL-10 concentrations by EIS

### 2.3.1. Preparation of working electrodes

Bare  $\text{HfO}_2$  substrates were cleaned and activated with TESUD (see Section 2.2). As  $\text{HfO}_2$  is an insulating material, the substrate functions on a charge effect as FETs. This differs in comparison to gold based biosensors where a charge transfer is obtained due to conductance of electron transfer using, for example, Fe(II/III) complex. Immobilization of the mAb was made in a conventional three-electrode glass cell for 2 h at  $4^\circ\text{C}$ , followed by rinsing with PBS. The measurement window for the  $\text{HfO}_2$  working electrode was calculated with an effective surface of  $\sim 0.50\ \text{cm}^2$ . Therefore, immobilization of the mAb and Ag were made with volumes of  $50\ \mu\text{L}$ . This ensured that all dilutions were maintained directly on the  $\text{HfO}_2$ . Measurements were made with a platinum plate counter electrode, and a silver/silver chloride ( $\text{Ag}/\text{AgCl}$ ) reference electrode (Radiometer Analytical, France). All measurements were made with freshly prepared PBS solution that required 10 mL to fill the cell,

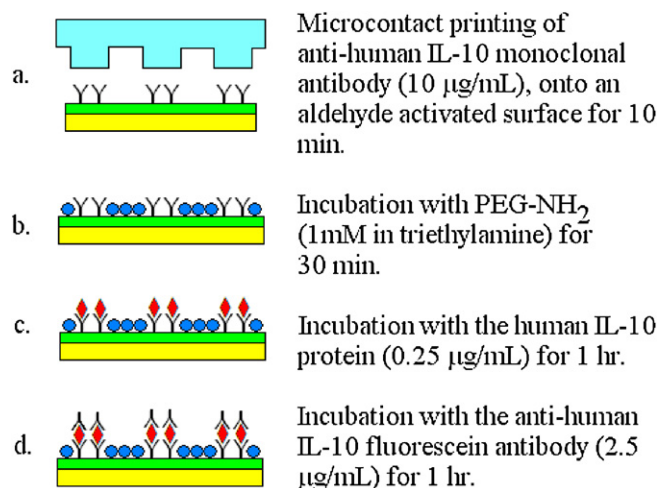


Fig. 2. Scheme for the activation of  $\text{HfO}_2$  for Ab–Ag–Ab bio-recognition of human IL-10 for fluorescence detection.

**Table 1**  
Contact angles of cleaned substrates, UV/Ozone activation, followed by TESUD formation on HfO<sub>2</sub>.

		
77 ± 1°	11 ± 2°	74 ± 1°
Cleaned HfO <sub>2</sub>	UV/Ozone activation	TESUD vapor phase

while the analysis was performed inside a Faraday cage. First, the IL-10 capture mAb were measured at a fixed potential that formulated a classical Nyquist curve using a VMP3 Bio-Logic Science Instrument, France. The preliminary plot established the required potential on the HfO<sub>2</sub> substrate. Starting from the lowest, varying human IL-10 concentrations were added after each analysis (30 min incubation at 4 °C). Finally, the frequency range was made from 200 mHz to 200 kHz, and an amplitude of 200 mV with a polarization potential of -2 V. The scan time was 35 s/scan. EC-Lab V10.18 modeling software (Bio-Logic Science Instrument, France) was applied to analyze the impedance data. For the Z-fit, the Nyquist plots were observed with Randomize+Simplex method, with randomize stopped on 100,000 iterations and the fit stopped on 5000 iterations.

### 3. Results and discussion

#### 3.1. Surface characterization of TESUD functionalization

By exposing HfO<sub>2</sub> to TESUD, SAMs of silane spontaneously absorb to the surface that leaves active aldehyde groups from the hydrocarbon chain positioned for reactivity toward the anti-human IL-10 mAb.

Contact angles were measured by analyzing a cleaned substrate, UV/Ozone activated, followed by TESUD functionalization. Measurements were made using a GBX Scientific Instruments (France) with Milli-Q water. Six values were recorded on each substrate, with 1 μL of ultrapure water deposited at 24 ± 2 °C.

The results in Table 1, demonstrate a slightly hydrophilic nature on HfO<sub>2</sub> at 77 ± 1°. Upon surface activation with UV/Ozone, HfO<sub>2</sub> became highly hydrophilic at 11 ± 2°. The *K* value of HfO<sub>2</sub> is 25 [21] and thus highly polar. As shown in accordance with the *K* value of HfO<sub>2</sub>, upon activation this surface increased in polarity. Therefore, with an improved *K*, this enabled increased saturation of the substrate to formulate well-organized SAMs of aldehyde-silane.

By vapor-phase with TESUD, the angle on HfO<sub>2</sub> increased in hydrophobicity, due to the formation of available aldehyde groups and hydrocarbon chains. This suggests that SAMs of TESUD have formulated due to a recorded value of 74 ± 1°. Finally, the functionalization of TESUD was assumed homogenous due to a small standard deviation (Fig. 3).

#### 3.2. Human IL-10 detection by direct patterning

Fluorescent imaging is a rapid tool for analyzing bio-layers, which ensures detection can be made by formulating bio-recognition processes due to the high affinity an Ab has for its corresponding Ag. The soft-lithographical technique, μCP, facilitates the printing of the required pattern by applying a structured PDMS stamp. The functionality of the immobilized receptor by the fluorescent pattern visible in Fig. 4, shows the formation of the Ab–Ag–Ab bio-recognition for human IL-10. The labeled fluorescent tags formulate positive structures, where non-printed regions have been blocked with PEG-NH<sub>2</sub>. Well-proportioned 10 μm<sup>2</sup> positive patterns are shown with perfectly immobilized IL-10 mAb, and this verified the covalent bonding of the

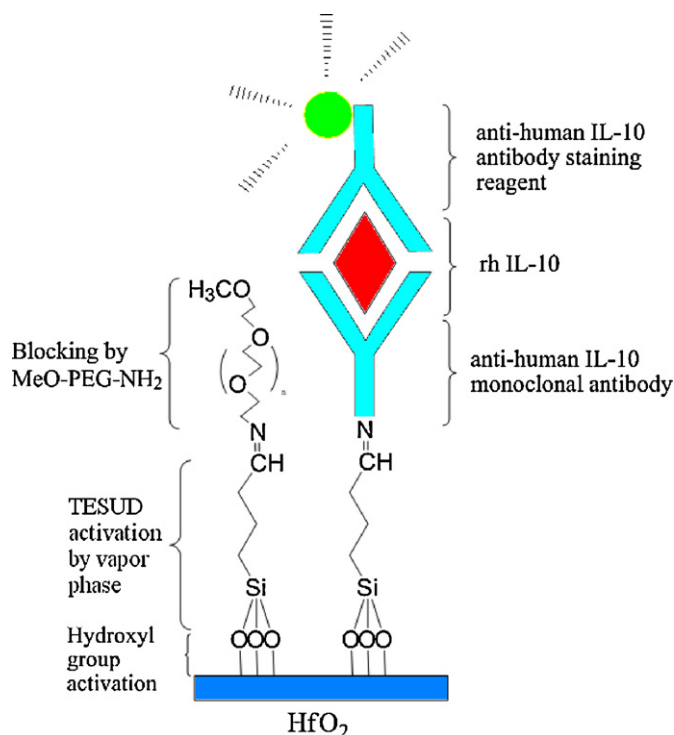


**Fig. 3.** Chemical mechanism for the formation of PEG-NH<sub>2</sub> blocking layer followed by the Ab–Ag–Ab bio-recognition of human IL-10.

anti-human capture mAb with a SAMs of aldehyde for direct patterning.

#### 3.3. EIS characterization with varying human IL-10 concentrations

EIS is an effective and efficient technique for investigating interfacial properties on surface modified working electrodes. Previous EIS results have indicated a distinction between the SAMs formation of the aldehyde when compared to bare HfO<sub>2</sub>. By covalent bonding of the Ab onto the surface, we followed the detection of the protein by Nyquist plots (Fig. 5). With incubation of the protein to form an Ab–Ag complex, the substrate shows a stepwise

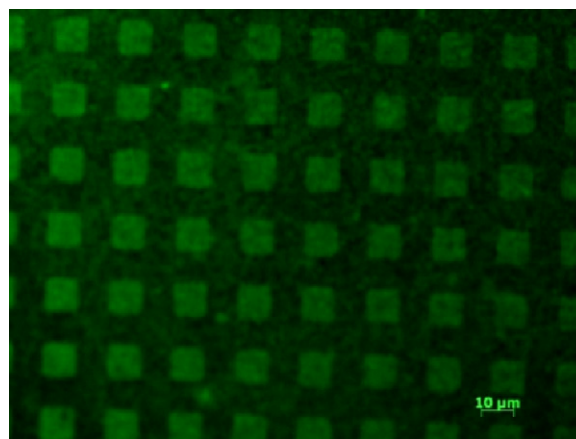


**Fig. 4.** Fluorescent image of IL-10 Ab–Ag–Ab recognition on HfO<sub>2</sub> using a positive 10 μm PDMS stamp using an automated μCP machine. After formation of the aldehyde layer, IL-10 mAb was μCP onto the surface, blocked with PEG-NH<sub>2</sub>, then incubated with human IL-10, followed by the IL-10 Ab tagged with fluorescein. The objective was taken at 50×.

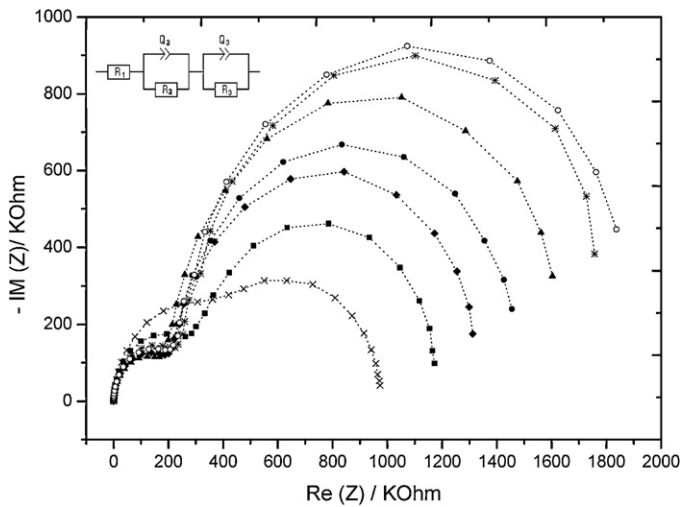


**Fig. 5.** Nyquist plot demonstrating detection of varying rh IL-10 concentrations in comparison with the IL-10 Ab. EIS measurements were carried out in PBS using the conditions: frequency range from 200 MHz to 200 kHz, an amplitude of 200 mV with a potential of  $-2$  V. ( $\times$ ) IL-10 Ab ( $10 \mu\text{g/mL}$ ) with human IL-10 at: ( $\blacksquare$ )  $0.1 \text{ pg/mL}$ ; ( $\blacklozenge$ )  $1 \text{ pg/mL}$ ; ( $\bullet$ )  $5 \text{ pg/mL}$ ; ( $\blacktriangle$ )  $20 \text{ ng/mL}$ ; ( $\text{⌘}$ )  $1 \text{ ng/mL}$ ; ( $\circ$ )  $50 \text{ ng/mL}$ . Inset: equivalent circuit applied for normalization.

formation in  $R_p$ , with detectable concentrations ranging from  $0.1 \text{ pg/mL}$  to  $50 \text{ ng/mL}$ .

The EIS of  $\text{HfO}_2$  modified with IL-10 mAb, followed by increasing human IL-10 protein concentrations were analyzed. A variation increase of the  $R_p$  can be seen from the initial IL-10 mAb (Fig. 5, plot  $\times$ ) at  $556 \text{ k}\Omega$  to human IL-10 ( $0.1 \text{ pg/mL}$ ,  $\blacksquare$ ) at  $898 \text{ k}\Omega$ . The change in resistance demonstrates the bio-recognition of the Ag to the fixed mAb on the  $\text{HfO}_2$  substrate. The  $R_p$  for human IL-10 increased with  $1 \text{ pg/mL}$  at  $1.2 \times 10^6 \text{ k}\Omega$  ( $\blacklozenge$ );  $5 \text{ pg/mL}$  at  $1.3 \times 10^6 \text{ k}\Omega$  ( $\bullet$ );  $20 \text{ pg/mL}$  at  $1.5 \times 10^6 \text{ k}\Omega$  ( $\blacktriangle$ );  $1 \text{ ng/mL}$  at  $1.7 \times 10^6 \text{ k}\Omega$  ( $\text{⌘}$ ); and  $50 \text{ ng/mL}$  at  $1.8 \times 10^6 \text{ k}\Omega$  ( $\circ$ ). The stepwise formation due to resistance, demonstrated that functionalization on  $\text{HfO}_2$  was achievable as this permitted the immobilization of the IL-10 mAb onto the  $\text{HfO}_2$  surface. The  $\sim 342 \text{ k}\Omega$  variations between the IL-10 mAb and the human IL-10 at  $0.1 \text{ pg/mL}$ , demonstrates that the biosensor was sensitive to this minute concentration. Detection from  $0.1 \text{ pg/mL}$  to  $50 \text{ ng/mL}$  increased within  $R_p$ , forming a clear distinction between each observable concentration analyzed. Here, we have established that detection was possible on this novel substrate with saturation occurring between  $1$  and  $50 \text{ ng/mL}$ .

Due to the thin layer of  $\text{HfO}_2$  at  $10.7 \text{ nm}$ , rejuvenation of the substrate was not possible due to the silanized layer. Repeated UV/Ozone can diminish the  $\text{HfO}_2$  layer, while Piranha will only remove the metal oxide and aluminum conducting layer. Also, since EIS is a highly sensitive technique reproducibility on the same  $\text{HfO}_2$  substrate was not desirable. However, to validate the biosensors response the experiment was repeated several times on different  $\text{HfO}_2$  substrates by applying the same conditions. The overall relative standard deviation percentage (%RSD) was  $7.33\%$  which proves the reproducibility of the biosensor.

From the impedance spectra, calculation of the fitting parameters applying an equivalent circuit can quantify the biosensor based on  $\text{HfO}_2$  (Table 2). This applies the variation of the  $R_p$  vs. rh IL-10 based in PBS. The equivalent electrical circuit ( $R_1 + Q_2/R_2 + Q_3/R_3$ ) applied for the simulation that formulated the best fit for the data is shown as the inset in Fig. 5. Here, the components can be explained as follows:  $R_1$  expresses the electrolyte solution ( $R_s$ ).  $Q_2$  is the constant phase element (CPE) ( $Q_{\text{sigma}2}$  and  $Q_{\text{alpha}2}$ ) that is parallel with  $R_2$  which is the  $R_p$  for the first Nyquist semi-circle. Finally,  $Q_3$  is another CPE ( $Q_{\text{sigma}3}$  and  $Q_{\text{alpha}3}$ ) which is parallel with

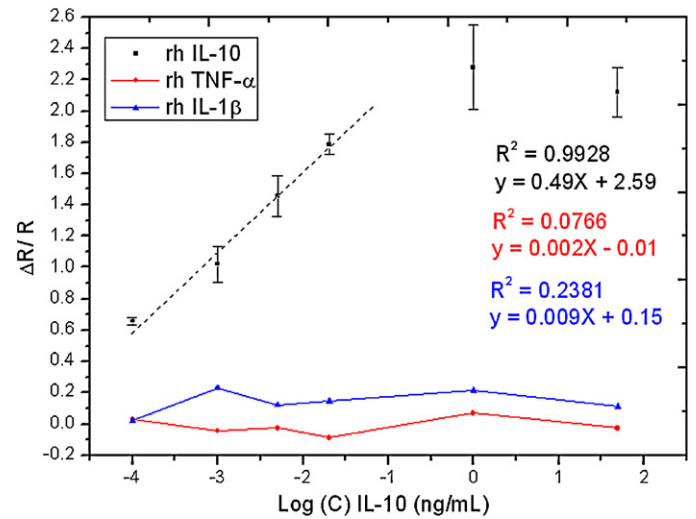


**Fig. 6.** Normalized curve by EIS detection of the logarithm of (black) rh IL-10 and selectivity of (red) rh TNF- $\alpha$  and (blue) rh IL- $1\beta$  with concentrations ranging from  $0.1 \text{ pg/mL}$  to  $50 \text{ ng/mL}$  against the variation of the  $R_p$  calculated by  $\Delta R/R$ . (For interpretation of the references to color in this figure legend, the reader is referred to the web version of the article.)

$R_3$  which is the  $R_p$  for the second Nyquist semi-circle. Therefore, the calculations of  $\Delta R/R$  were made with  $R_3$  (due to the formation of two compressed semi-circles in the Nyquist plot, the imperfect capacitors of CPE functioned with improved fitting values when compared to pure capacitive components ( $C_2$  and  $C_3$ )). In Fig. 6 (black), the  $R_p$  and the logarithm of the rh IL-10 concentration (C) plot produced a linear relationship ranging from  $0.1 \text{ pg/mL}$  to  $20 \text{ pg/mL}$  at  $R^2 = 0.9928$  with a sensitivity of  $0.49 \text{ (ng/mL)}^{-1}$ . Values for NYHA classify HF patients rh IL-10 values between  $\sim 0$  and  $10 \text{ pg/mL}$  for NYHA class I/II and III/IV. However, from literature we have previously seen that these values are dependent upon pre- and post-implantation of LVAD, since an increase of IL-10 was observed after surgery. At present, with our detectable concentration, the novel biosensor was capable of measuring at this concentration requirement (e.g. non-survivors between  $0$  and  $4 \text{ h}$  recorded values of  $5.6\text{--}177.8 \text{ pg/mL}$  of IL-10 [2]). From  $0.1 \text{ pg/mL}$  to  $1 \text{ ng/mL}$ , the biosensor began to saturate as the linearity was reduced to  $R^2 = 0.9889$  with a sensitivity of  $0.42 \text{ (ng/mL)}^{-1}$ , while, from  $1 \text{ ng/mL}$  to  $50 \text{ ng/mL}$ , the biosensor was saturated with human IL-10.

The level of interference attributable to non-specific binding of inactive proteins were analyzed with the cytokines; TNF- $\alpha$ , and IL- $1\beta$  which are other prevalent biomarkers relevant to LVAD recipients. Here, the same conditions and concentrations were applied as rh IL-10. Applying a  $\text{HfO}_2$  substrate with a monolayer of anti-human IL-10 mAb, we analyzed the interference of rh TNF- $\alpha$  and rh IL- $1\beta$ . On calculation of the fitting parameters, we see in Fig. 6, preliminary results for the selectivity of the biosensor. The detection of rh IL-10 demonstrates linearity upon increasing the concentration until the point of saturation. Reduced  $\Delta R/R$  values significant to rh TNF- $\alpha$  (red) ( $R^2 = 0.0766$  with a sensitivity of  $0.002 \text{ (ng/mL)}^{-1}$ ) and rh IL- $1\beta$  (blue) ( $R^2 = 0.2381$  with a sensitivity of  $0.009 \text{ (ng/mL)}^{-1}$ ), demonstrates the sensitivity was considerably lower in comparison to human IL-10. For instance, in comparison toward rh TNF- $\alpha$ , the biosensor was  $245$  times more selective with rh IL-10, and  $54$  times more selective with rh IL-10 when compared to rh IL- $1\beta$ . Here, we have established by EIS that selectivity was sensitive to only human IL-10.

Undoubtedly, the gold standard for the quantification of cytokines is by ELISA technique, however, immobilization, bio-conjugation, wash steps, and quantification requires increased time

**Table 2**  
Fitting parameters obtained from the equivalent circuit of the human IL-10 based HfO<sub>2</sub> biosensor.

Ag conc.	R <sub>1</sub> (Ω)	Q <sub>2</sub> (nF·s <sup>(a-1)</sup> )	R <sub>2</sub> (kΩ)	Q <sub>3</sub> (nF·s <sup>(a-1)</sup> )	R <sub>3</sub> (kΩ)	χ <sup>2</sup>
0 pg/mL	362.2 ± 0.3	13.230 ± 0.001	413.51 ± 0.02	82.070 ± 0.005	556.28 ± 0.02	0.0042
0.1 pg/mL	389.5 ± 0.3	10.090 ± 0.001	296.35 ± 0.01	107.900 ± 0.001	898.0430 ± 0.0003	0.0124
1 pg/mL	361.7 ± 0.3	10.020 ± 0.001	216.391 ± 0.004	114.500 ± 0.001	1161 ± 0.001	0.0188
5 pg/mL	366.9 ± 0.3	10.450 ± 0.001	218.099 ± 0.004	115.500 ± 0.001	1308 ± 0.002	0.0196
20 pg/mL	358.9 ± 0.3	10.400 ± 0.001	197.575 ± 0.003	118.300 ± 0.001	1523 ± 0.001	0.0268
1 ng/mL	383.2 ± 0.3	9.874 ± 0.001	249.532 ± 0.003	119.100 ± 0.001	1727 ± 0.004	0.0295
50 ng/mL	376.9 ± 0.3	11.760 ± 0.001	231.840 ± 0.003	122.300 ± 0.001	1822 ± 0.005	0.0282

and input from qualified personnel. The ELISA kits are designed for accuracy at a sensitivity of ~3 pg/mL with the detectable assay range made at higher concentrations e.g. 15.4–600 pg/mL [30–32]. However, lower concentrations can be detected with high sensitivity though at a reduced dynamic range. The drawback of ELISA kits is that they have short usability time due to the lyophilized components, and if applied immediately following sample collection to data acquisition, ELISA kits can take over half a day to have a definitive reading. Depending upon the cost and resources of a clinical laboratory, samples may be collected and frozen until a sufficient amount has been obtained from multiple patients. Therefore, the time of analysis is ultimately delayed, and specific knowledge affordable to protein concentration during the first few hours after implantation cannot be deduced hastily. In due course, this will prevent adequate therapeutic intervention when the patients' clinical status requires it the most. As a consequence, this demonstrates the possible alternative application of biosensors for real-time detection of inflammatory status during the early phase of LVAD implantation. A biosensor can be manufactured at reduced costs, preparation time (where no label or multiple wash steps are required), and reduced analysis time.

#### 4. Conclusions

In this study, we have achieved surface functionalization of HfO<sub>2</sub> by formulating SAMs of TESUD by vapor-phase in a saturated medium. Surface modification on HfO<sub>2</sub> has enabled covalent bonding with the Ab and demonstrated the effectiveness, since aldehyde formation permitted direct patterning of anti-human IL-10 mAb onto HfO<sub>2</sub> by μCP. The patterned mAb had affinity to the human protein and was observed by a secondary fluorescent Ab. EIS has shown that detection could be made with varying human IL-10 concentrations within the pico- to nano-gram range. Here, for increased sensitivity the detectable limit was analyzed from 0.1 pg/mL. The increment of the dynamic range to larger concentrations can express the high risk of MOFS as a direct cause to implantation. To our knowledge, this is the first novel biosensor that has been based on HfO<sub>2</sub> for protein detection by means of EIS.

IL-10 is one of many cytokines that can discriminate patients at a high risk of MOFS development, and biosensors in the form of point-of-care devices may present a valuable tool for evaluation of inflammatory status after LVAD implantation. Quantification is rapid and this can enhance the therapeutic intervention in an intensive care unit, thus increasing the survival rate of patients by means of early detection of an altered inflammatory process, as evidenced by excessive release of circulating anti-inflammatory cytokines.

Work is on-going to optimize all conditions for this novel substrate, while future applications will concentrate on the development of biosensors based on FETs using HfO<sub>2</sub> as a gate. Analysis of biological samples (e.g. plasma) will then determine the limit

of detection, linearity, response time, and sensitivity of this novel HfO<sub>2</sub> biosensor.

#### Acknowledgments

We acknowledge the funding through the Ministère de L'enseignement Supérieur et de la Recherche (MESR) and from the SensorART project, funded by the European Communities Seventh Framework Programme (FP7/2007–2013) under the grant agreement No. 248763, and from InFuLOC project under grant agreement No. 230749.

#### References

- [1] K.G.J. Ooi, G. Galatowicz, H.M.A. Towler, S.L. Lightman, V.L. Calder, Multiplex cytokine detection versus ELISA for aqueous humor: IL-5, IL-10, and IFNγ profiles in uveitis, *Investigative Ophthalmology and Visual Science* 47 (2006) 272–277.
- [2] R. Caruso, S. Trunfio, F. Milazzo, J. Campolo, R. De Maria, T. Colombo, M. Parolini, A. Cannata, C. Russo, R. Paino, M. Frigerio, L. Martinelli, O. Parodi, Early expression of pro- and anti-inflammatory cytokines in left ventricular assist device recipients with multiple organ failure syndrome, *American Society for Artificial Internal Organs Journal* 56 (2010) 313–318.
- [3] R. Caruso, A. Verde, M. Cabiati, F. Milazzo, C. Boroni, S. Del Ry, M. Parolini, C. Vittori, R. Paino, L. Martinelli, D. Giannessi, M. Frigerio, O. Parodi, Association of pre-operative interleukin-6 levels with interagency registry for mechanically assisted circulatory support profiles and intensive care unit stay in left ventricular assist device patients, *Journal of Heart and Lung Transplantation*, in press.
- [4] C.J. Watson, M.T. Ledwidge, D. Phelan, P. Collier, J.C. Byrne, M.J. Dunn, K.M. McDonald, J.A. Baugh, Proteomic analysis of coronary sinus serum reveals leucine-rich α2-glycoprotein as a novel biomarker of ventricular dysfunction and heart failure, *Circulation: Heart Failure* 4 (2011) 188–197.
- [5] M. Maurer, S. Burri, S. de Marchi, R. Hullin, M. Martinelli, P. Mohacs, O.M. Hess, Plasma homocysteine and cardiovascular risk in heart failure with and without cardiorenal syndrome, *International Journal of Cardiology* 141 (2010) 32–38.
- [6] M. Hnaien, F. Lagarde, J. Bausells, A. Errachid, N. Jaffrezic-Renault, A new bacterial biosensor for trichloroethylene detection based on a three-dimensional carbon nanotubes bioarchitecture, *Analytical and Bioanalytical Chemistry* 400 (2011) 1083–1092.
- [7] J. Vidic, M. Pla-Roca, J. Grosclaude, M.A. Persuy, R. Monnerie, D. Caballero, A. Errachid, Y. Hou, N. Jaffrezic-Renault, R. Salesse, E. Pajot-Augy, J. Samitier, Gold surface functionalization and patterning for specific immobilization of olfactory receptors carried by nanosomes, *Analytical Chemistry* 79 (2007) 3280–3290.
- [8] S. Bourigou, M. Hnaien, F. Bessueille, F. Lagarde, S. Dzyadevych, A. Maaref, J. Bausells, A. Errachid, N. Jaffrezic Renault, Impedimetric immunosensor based on SWCNT-COOH modified gold microelectrodes for label-free detection of deep venous thrombosis biomarker, *Sensors and Bioelectronics* 26 (2010) 1278–1282.
- [9] S. Chebil, I. Hafaidh, H. Sauriat-Dorizon, N. Jaffrezic-Renault, A. Errachid, Z. Ali, H. Korri-Youssoufi, Electrochemical detection of D-dimer as deep vein thrombosis marker using single-chain d-dimer antibody immobilized on functionalized polypyrrole, *Sensors and Bioelectronics* 26 (2010) 736–742.
- [10] S. Hleli, C. Martelet, A. Abdelghani, F. Bessueille, A. Errachid, J. Samitier, H.C.W. Hays, P.A. Millner, N. Burais, N. Jaffrezic-Renault, An immunosensor for haemoglobin based on impedimetric properties of a new mixed self-assembled mono layer, *Materials Science and Engineering Research C* 26 (2006) 322–327.
- [11] T. Li, M. Yang, Electrochemical sensor utilizing ferrocene loaded porous polyelectrolyte nanoparticles as label for the detection of protein biomarker IL-6, *Sensors and Actuators B* 158 (2011) 361–365.
- [12] B.S. Munge, A.L. Coffey, J.M. Doucette, B.K. Somba, R. Malhotra, V. Patel, J.S. Gutkind, J.F. Rusling, Nanostructured immunosensor for attomolar detection of cancer biomarker interleukin-8 using massively labeled superparamagnetic particles, *Angewandte Chemie International Edition* 50 (2009) 7915–7918.

- [13] J. Wang, Electrochemical biosensors: towards point-of-care cancer diagnostics, *Biosensors and Bioelectronics* 21 (2006) 1887–1892.
- [14] M. Castellarnau, N. Zine, J. Bausells, C. Madrid, A. Juárez, J. Samitier, A. Errachid, Integrated cell positioning and cell-based ISFET biosensors, *Sensors and Actuators B* 120 (2007) 615–620.
- [15] J. Gustavsson, G. Altankov, A. Errachid, J. Samitier, J. Planell, E. Engel, Surface modifications of silicon nitride for cellular biosensor applications, *Journal of Materials Science: Materials in Medicine* 19 (2008) 1839–1850.
- [16] I.A. Marques de Oliveira, D. Caballero, Z.M. Baccar, Z. Mazzouz, R. Eritja, N. Zine, J. Samitier, A. Errachid, Immobilization of DNA on silicon nitride by microcontact printing: characterisation of DNA-IS sensors by atomic force microscopy and impedance spectroscopy methods, in: XIXth International Symposium on Bioelectrochemistry and Bioenergetics, Toulouse (France), April, 2007.
- [17] A. Amari, N. El Bari, N. Zine, D. Caballero, B. Bouchikhi, A. Errachid, Nanocharacterization of a novel biosensor sensitive to beta casein using AFM and impedance spectroscopy, in: Euroensors XXII, Dresden (Germany), September, 2008.
- [18] R. Garg, HfO<sub>2</sub> as gate dielectric on Si and Ge substrate, Ph.D. Thesis, New Jersey's Science & Technology University (NJIT), USA, 2006.
- [19] J.M. Rafi, M. Zabala, O. Beldarrain, F. Campabadal, Effect of processing conditions on the electrical characteristics of atomic layer deposited Al<sub>2</sub>O<sub>3</sub> and HfO<sub>2</sub> films, *ESC Transactions* 28 (2010) 213–221.
- [20] F. Campabadal, J.M. Rafi, M. Zabala, O. Beldarrain, Electrical characteristics of metal-insulator-semiconductor structures with atomic layer deposited Al<sub>2</sub>O<sub>3</sub>, HfO<sub>2</sub>, and nanolaminates on different silicon substrates, *Journal of Vacuum Science and Technology B* 23 (2011), <http://dx.doi.org/10.1116/1.3532544>.
- [21] G.D. Wilk, R.M. Wallace, J.M. Anthony, High-k gate dielectrics: current status and materials properties considerations, *Journal of Applied Physics* 89 (2001) 5243–5275.
- [22] T.J. Park, J.H. Kim, J.H. Jang, C-K. Lee, K.D. Na, S.Y. Lee, H-S. Jung, M. Kim, S. Han, C.S. Hwang, Reduction of electrical defects in atomic layer deposited HfO<sub>2</sub> films by Al doping, *Chemistry of Materials* 22 (2010) 4175–4184.
- [23] J.F. Kang, H.Y. Yu, C. Ren, M-F. Li, D.S.H. Chan, H. Hu, H.F. Lim, Thermal stability of nitrogen incorporated in HfN<sub>2</sub>O<sub>2</sub> gate dielectrics prepared by reactive sputtering, *Applied Physics Letters* 84 (2004) 1588–1590.
- [24] S.J. Lee, H.F. Luan, W.P. Bai, C.H. Lee, T.S. Jeon, Y. Senzaki, D. Roberts, D.L. Kwong, High quality ultra thin CVD HfO<sub>2</sub> gate stack with poly-Si gate electrode, *Technical Digest: International Electron Devices Meeting* (2000) 31–34.
- [25] Y.W. Chen, M. Liu, T. Kaneko, P.C. McIntyre, Atomic layer deposited hafnium oxide gate dielectrics for charge-based biosensors, *Electrochemical and Solid State Letters* 13 (2010) G29–G32.
- [26] C. Stumpf, C. Lehner, A. Yilmaz, W.G. Daniel, C.D. Garlichs, Decrease of serum levels of the anti-inflammatory cytokine interleukin-10 in patients with advanced chronic heart failure, *Clinical Science* 105 (2003) 45–50.
- [27] A.P. Bolger, R. Sharma, S. von Haehling, W. Doehner, B. Oliver, M. Rauchhaus, A.J.S. Coats, I.M. Adcock, S.D. Anker, Effect of Interleukin-10 on the production of tumour necrosis factor- $\alpha$  by peripheral blood mononuclear cells from patients with chronic heart failure, *American Journal of Cardiology* 90 (2002) 384–389.
- [28] D. Caballero, J. Samitier, J. Bausells, A. Errachid, Direct patterning of anti-human serum albumin antibodies on aldehydeterminated silicon nitride surfaces for HSA protein detection, *Small* 5 (2009) 1531–1534.
- [29] D. Caballero, E. Martinez, J. Bausells, A. Errachid, J. Samitier, Impedimetric immunosensor for human serum albumin detection on a direct aldehyde-functionalized silicon nitride surface, *Analytica Chimica Acta* 720 (2012) 43–48.
- [30] Quantikine® ELISA Human IL-10 Immunoassay, © 2011, R&D Systems, Inc., <http://www.rndsystems.com/pdf/d1000b.pdf>.
- [31] Human IL-10 Colorimetric ELISA Kit, © 2012, Thermo Fisher Scientific Inc., <http://www.piercenet.com/browse.cfm?fidID=07010143>.
- [32] IL-10 Human ELISA Kit, © 1998–2012, Abcam plc., <http://www.abcam.com/IL10-Human-ELISA-Kit-2-x-96-Well-Plates-ab46057.html>.

## Biographies

**Michael Lee** received his B.S. in forensic science from Northumbria University in 2004 and his M.S. in analytical chemistry at Teesside University in 2006. He is currently a Ph.D. student in the group of Prof. Abdelhamid Errachid.

**Dr. Nadia Zine** received her B.S. in chemistry from the University M. Ismail, Meknes in 1994 and her Ph.D. from the Centro Nacional de Microelectrónica (CNM) Barcelona in 2005. Currently, she is a lecturer/researcher at the Claude Bernard University-Lyon 1. Her research interest is the chemical characterization of silicon chemical sensors, and specially, of ISFET devices.

**Abdellatif Baraket** received his B.S. in physics and M.S. in scientific computing in physics and experimental high energy from Hassan 2 University in 2006 and 2008 respectively. He also received a M.S. in physics and nanomaterial from the University of Maine in 2009. He is currently a Ph.D. student in the group of Prof. Abdelhamid Errachid.

**Miguel Zabala** graduated in telecommunications engineering at the Universitat Politècnica de Catalunya, Barcelona, in 1995. In 1995, he joined the Centro Nacional de Microelectronica (CNM) where he is currently working. His main area of interest is thermal process engineering for nano-microelectronic technologies and analog circuitry for microsystems.

**Dr. Francesca Campabadal** received her Ph.D. degree in physics in 1986 from the Universitat Autònoma de Barcelona. In 1987 she joined CNM, working on thin oxide technology and characterization. Since 1992, her research activities have been also in the field of technologies for the monolithic integration of mechanical sensors and CMOS circuitry and pressure sensor packaging.

**Dr. Raffaele Caruso** graduated in biological sciences at the University of Milan in 1995 and he majored in Biochemical and Clinical Chemistry in 2002. He is an Investigator of Italian National Research Council (CNR), and since 2005, his main activities have been in the field of the inflammatory pathways affecting the clinical outcome in ESHF patients supported by LVAD, and in ventricular remodeling.

**Dr. Maria Giovanna Trivella** received her medical doctor degree from the University of Pisa in 1976 and she majored in Cardiology in 1981. She is a senior investigator of Italian National Research Council (CNR), head of Experimental Laboratory of IFC-CNR and head of Experimental Surgery Laboratory, a joint laboratory in cooperation between CNR and University of Pisa. Awarded in 2007 by the European Science Foundation for the Exploratory Workshop “molecular signaling in cardiovascular and oncological disease: similar and shared pathways”. The current research fields of interest are interdisciplinary and translational research in medicine. She is the coordinator of SensorART – a remote controlled sensorized artificial heart enabling patients empowerment and new therapy approaches (FP7-ICT-248763), 2010–2014.

**Dr. Nicole Jaffrezic-Renault** received her engineering degree from the Ecole Nationale Supérieure de Chimie, Paris, in 1971 and the Doctorat d'Etat és Sciences Physiques from the University of Paris in 1976. She joined Ecole Centrale de Lyon, France in 1984 and Claude Bernard University-Lyon 1 in 2007. As director of research at the Center National de la Recherche Scientifique and the president of the chemical microsensor club (CMC2), her research activities include the conception and fabrication of chemical and bio-sensors based on microtransducers (ISFETs, optical fiber sensors, electrochemical sensors) and on nanomaterials.

**Prof. Abdelhamid Errachid** graduated in physics from the University M. Ismail, Meknes, 1992 and received a Ph.D. degree in electronic engineering from the Universitat Autònoma de Barcelona, Spain, in 1998. Since 2008, he had joined Laboratory of Analytical Sciences in Claude Bernard University-Lyon 1 as a full professor. He is now involved in several national and European projects. His current research activity is focused on bioelectronics, biofunctionalization and nanobiotechnology.